PHYSICS AND CHEMISTRY OF SOLID STATE
V. 25, No. 1 (2024) pp. 65-72
Section: Physics

DOI: 10.15330/pcss.25.1.65-72

Vasyl Stefanyk Precarpathian National University

ФІЗИКА І ХІМІЯ ТВЕРДОГО ТІЛА
Т. 25, № 1 (2024) С. 65-72
Фізико-математичні науки

PACS: 71.15.Mb; 71.20. ± b; 71.20.Nr ISSN 1729-4428

S.V. Syrotyuk, A.Y. Nakonechnyi, Yu.V. Klysko, H.I. Vlakh-Vyhrynovska, Z.E. Veres

Electronic and magnetic properties of ZnSeS solid solution modified by Mn impurity, Zn vacancy and pressure

CAS Department, Lviv Polytechnic National University, Lviv, Ukraine. stepan.v.syrotiuk@lpnu.ua

The spin-polarized electronic energy spectra of the ZnSeS solid solution were obtained based on calculations for the supercell, which contains 64 atoms. At the *first* stage, the properties of the material based on the Mn:ZnSeS supercell, in which Mn replaces the Zn atom, were calculated. The calculation results reveal that the material is a semiconductor for both spin orientations. The *second* stage is based on the simultaneous presence of a Mn impurity and a cation vacancy. Comparing the results of the first two stages allows us to reveal significant changes in the electronic energy structure caused by the cation vacancy. The material with a vacancy exhibits metallic properties for both spin orientations. The *third* stage is implemented for the supercell without a vacancy, but under the action of hydrostatic pressure. The material exhibits semiconducting properties for both values of the spin moment. At the *fourth* stage, the Mn:ZnSeS supercell with a vacancy and under pressure is considered. In the presence of pressure and a V_{Zn} vacancy, the ZnMnSeS material exhibits metallic properties for both spin orientations. A material with a vacancy and under pressure can be characterized as a magnetic metal.

Keywords: AIIBVI Solid Solutions, Strongly Correlated Electrons, Energy Spectrum, Density of Electronic States.

Received 05 November 2023; Accepted 7 February 2024.

Introduction

Earlier, the possibility of obtaining scintillation materials based on mixed crystals (ZnS-ZnTe) has been shown [1]. These mixed crystals have found many applications, namely in development of detecting devices for introscopic systems and in multi-energy X-ray radiography [2]. The variation of the band gap width opens possibilities for obtaining ZnS-based materials with predetermined scintillation properties [3].

Obtaining of ZnS_xTe_{1-x} mixed crystals is difficult due to the limited solubility of their components and is possible only at 8–10% concentrations in accordance with the ZnS_xTe_{1-x} state diagram [4]. Among various AIIBVI solid solutions, $ZnSe_{1-x}S_x$ crystals are of especial interest. Unlimited ZnS-ZnSe mutual solubility makes possible obtaining of the $ZnSe_{1-x}S_x$ crystals with any x value [5].

Work [6] reports on α-ZnSe, α-ZnS and α-ZnS_xSe_{1-x} heterolayers obtained by the method of isovalent substitution. Thin layers of wide-gap II-VI semiconductors are widely used in various electronic devices. Among them, these devices are considered to be characterized by a number of properties favorable for use.

AIIBVI materials are intensively studied now within the framework of various theoretical approaches. In particular, the kinetic properties of the CdTe material were recently studied from the first principles in the formalism of projection augmented waves (PAW, projector augmented waves) [7]. The electronic, phonon, optical, and thermodynamic properties of the CdTe crystal were studied on the basis of the density functional theory (DFT) using the pseudopotential method [8]. The same theoretical approach was successfully applied to study the electronic structure of CdSeTe solid solutions [9].

Experiments with crystals II-VI with impurities of transition elements revealed materials, in particular Fe:ZnSe, suitable for the co-construction of lasers in the mid-infrared region of the spectrum [10]. ZnX chalcogenides (X = S, Se, Te) were devoted to a number of experimental and theoretical studies of their electronic and optical properties [11-14].

However, studies of II-VI solid solutions with impurities of transition elements are currently rare [15, 16]. These materials are also promising in terms of obtaining the nanostructures [17].

The purpose of this work is to study the influence of pressure and point defects, as well as the combined effect of these factors on the change in the electronic and magnetic properties of the Mn:ZnSeS crystal. Calculations were performed in a 2×2×2 supercell containing 64 atoms.

I. Theory and calculation details

The method of projection augmented waves (PAW, projector augmented waves) [18, 19] combines the features of the pseudopotential and the all-electronic approach of augmented plane waves. The wave $\Psi_n(r)$ and pseudo-wave $\widetilde{\Psi}_n(r)$ functions are related to each other as follows:

$$|\Psi_n(r)\rangle = |\widetilde{\Psi}_n(\mathrm{r})\rangle + \sum_a \sum_i (|\phi_i^a(r)\rangle - |\tilde{\phi}_i^a(r)\rangle)\,\langle\tilde{p}_i^a|\widetilde{\Psi}_n\rangle, \quad (1)$$

where $|\phi_i^a(r)\rangle$ is the atomic wave function, $|\tilde{\phi}_i^a(r)\rangle$ is the pseudo-wave function, and $\langle\tilde{p}_i^a|$ is the projector function. The summation in (1) is carried out over the augmentation spheres, which are numbered with the index *a*, and the index $i = \{n, l, m\}$ corresponds to the principal, orbital, and magnetic quantum numbers, respectively.

From equation (1) we see that

$$|\Psi_n(r)\rangle = \tau|\widetilde{\Psi}_n(\mathrm{r})\rangle, \quad (2)$$

where operator τ transforms the pseudo-wave function $|\widetilde{\Psi}_n(\mathrm{r})\rangle$, into an all-electronic state $\Psi_n(r)$

The explicit form of the operator follows from equation (1):

$$\tau = 1 + \sum_a \sum_i (|\phi_i^a(r)\rangle - |\tilde{\phi}_i^a(r)\rangle)\,\langle\tilde{p}_i^a|. \quad (3).$$

Stationary Schrödinger equation

$$H|\Psi_n\rangle = |\Psi_n\rangle\varepsilon_n\,, \quad (4)$$

taking into account (2), takes the following form:

$$\tau^+ H\tau|\widetilde{\Psi}_n\rangle = \tau^+\tau|\Psi_n\rangle\varepsilon_n\,, \quad (5)$$

in which the desired electron spectrum is the same as in equation (4).

The idea of the PAW method is to transform the Schrödinger equation into an equation in which the unknown state function is $|\widetilde{\Psi}_n\rangle$. If it is found, then with the help of (1) the entire electronic function of the state $|\Psi_n\rangle$ is obtained. Using the latter, we find the electron density and the corresponding Hartree potential.

The exchange-correlation potential was chosen in the PBE0 form [20, 21], according to which the exchange-correlation energy functional

$$E_{xc}^{PBE0}[\rho] = E_{xc}^{PBE}[\rho] + \tfrac{1}{4}(E_x^{HF}[\Psi_{3d}] - E_x^{PBE}[\rho_{3d}]), \quad (6)$$

where PBE corresponds to the exchange-correlation functional [20], and Ψ_{3d}, ρ_{3d} denote the wave function and electron density the Mn atom.

Exchange energy in the Hartree-Fock theory

$$E_x^{HF}[\Psi_{3d}] = -\tfrac{1}{2}\sum_{nn'}^{occ} \delta_{\sigma_n\sigma_{n'}} \int dr dr' \frac{\Psi_n(r)\Psi_{n'}^*(r)\Psi_n^*(r')\Psi_{n'}(r')}{|r-r'|}, \quad (7)$$

Where n, n' are the quantum numbers of correlated states occupied by electrons, and σ_n, $\sigma_{n'}$ are the corresponding spins.

Four variants of calculations were performed in 2×2×2 supercells using the Abinit program [18] in the PAW basis.

1. The Mn:ZnSeS supercell contains 64 atoms, and its formula unit is $Zn_{31}Mn_1Se_{24}S_8$, that is, one Zn atom is replaced by an Mn atom. Conditions are normal, i.e. pressure P = 0.

2. The supercell is taken from the previous point 1, but the external hydrostatic pressure P = 23 GPa.

3. The supercell contains 63 atoms, and its formula unit is Zn30Mn1Se24S8, i.e. there is a Zn vacancy, V_{Zn}. Pressure P = 0.

4. The supercell is taken from the previous point 3, but with the presence of external hydrostatic pressure P = 23 GPa.

First, the influence of the transition Mn 3d element impurity on the electronic structure of the ZnSeS material was studied, and then the changes in the electronic properties caused by the combined action of the substitution atom, external pressure, and the V_{Zn} point defect were revealed. The structure of the material was optimized by the minimizing the total energy as a function of the volume of the supercell. A spatial grid of 90×90×90 was used to calculate the wave function, and the more denser 125×125×125 grid was applied for evaluation of the electron density and crystal potential.

II. Results analysis

Figure 1 shows the spin-polarized electronic energy spectra of the Mn:ZnSeS crystal without and with Zn vacancy (V_{Zn}, vac). These results were obtained under ambient conditions, that is, in the absence of external pressure (P=0). A comparison of dispersion laws reveals a significant influence of the V_{Zn} vacancy on the electronic structure of the Mn:ZnSeS material for both spin orientations. In particular, if in the absence of defects the material is a semiconductor for both spin orientations, then

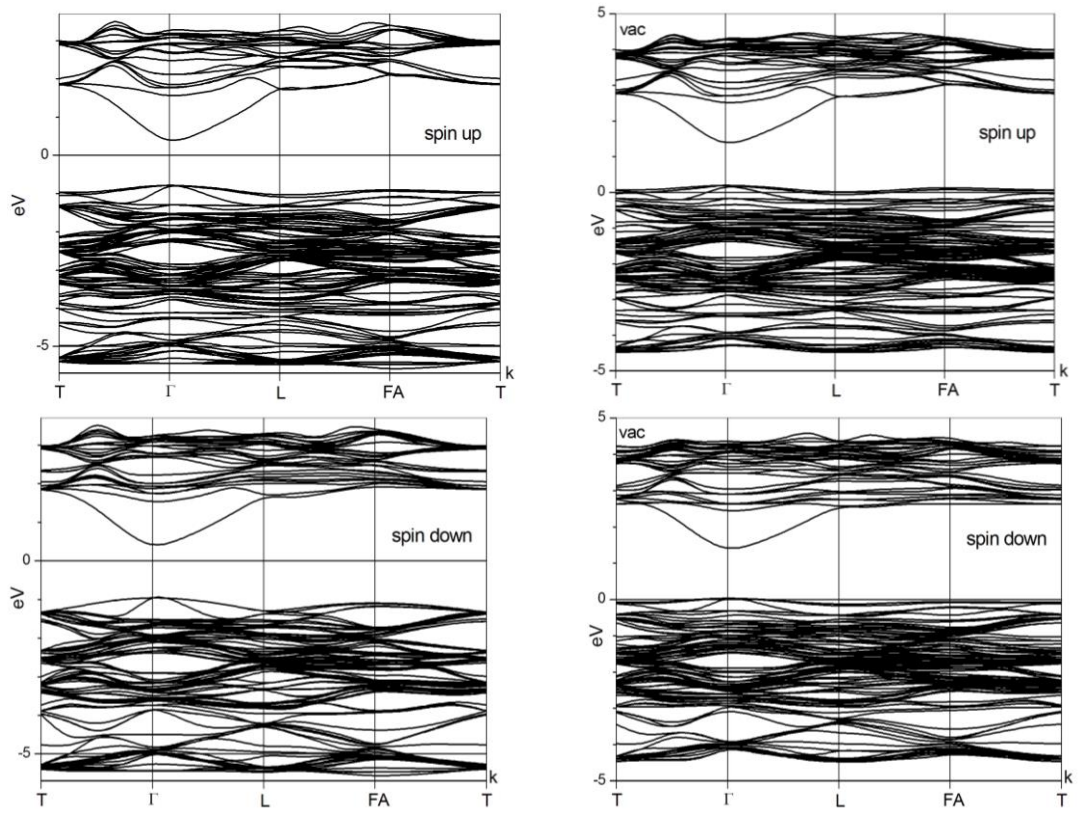

Fig. 1. Spin-polarized electronic energy spectra of the Mn:ZnSeS material without and with a V_{Zn} vacancy (vac). Pressure P = 0.

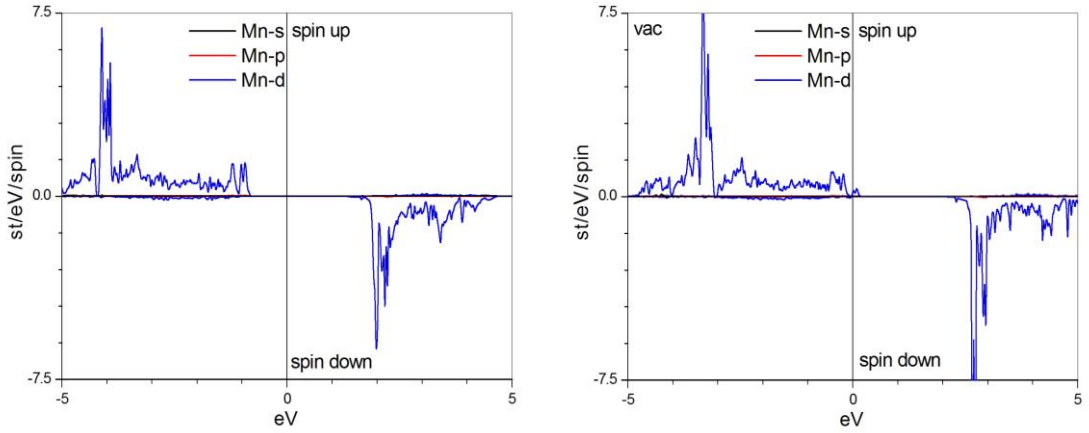

Fig. 2. The Mn partial density of electronic states in the Mn:ZnSeS material, without and with V_{Zn} vacancy. Pressure P = 0.

in the presence of vacancies it exhibits metallic properties. Indeed, the Fermi level in a material with defects is localized in the upper part of the valence band.

Figure 2 shows the spin-polarized densities of electronic states of Mn for an uncompressed crystal.

Mn:ZnSeS without a V_{Zn} vacancy and with the presence of the latter. We note that in a material with defects (vac), the Fermi level crosses the density of states of 3d symmetry of electrons with spins up.

Figure 3 shows the spin-polarized partial densities of electronic states of Zn in the Mn:ZnSeS material, found under normal conditions. We note that in the material with point defects (vac) the electronic states of Zn are present at the Fermi level.

In Fig. 4 are shown the spin-polarized partial densities of electronic states of Se in the Mn:ZnSeS material, calculated under normal conditions. The curves of the density of states for the material with defects (vac) reveal the presence of the Se p states at the Fermi level for both values of the spin moment.

Figure 5 shows the spin-polarized partial densities of electronic states on the S atom in the Mn:ZnSeS material, calculated under ambient conditions. The curves of the density of states for the material with defects (vac) reveal a significant presence of the atom S p states at the Fermi level for both values of the spin moment.

In Fig. 6 are presented the spin-polarized electronic energy spectra of the Mn:ZnSeS crystal without the Zn vacancy (V_{Zn}) and with last one (vac). These results were found in the presence of an external pressure of

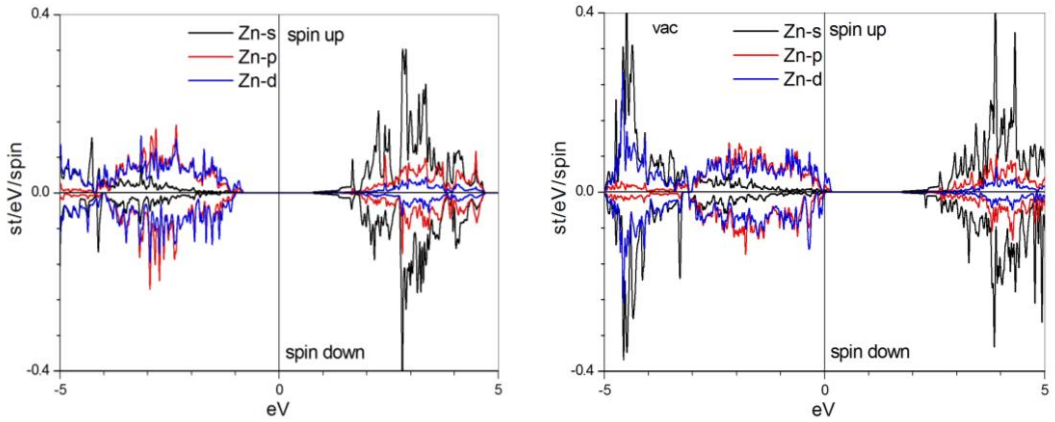

Fig. 3. The Zn partial density of electronic states in the Mn:ZnSeS material, without and with V_{Zn} vacancy. Pressure P = 0.

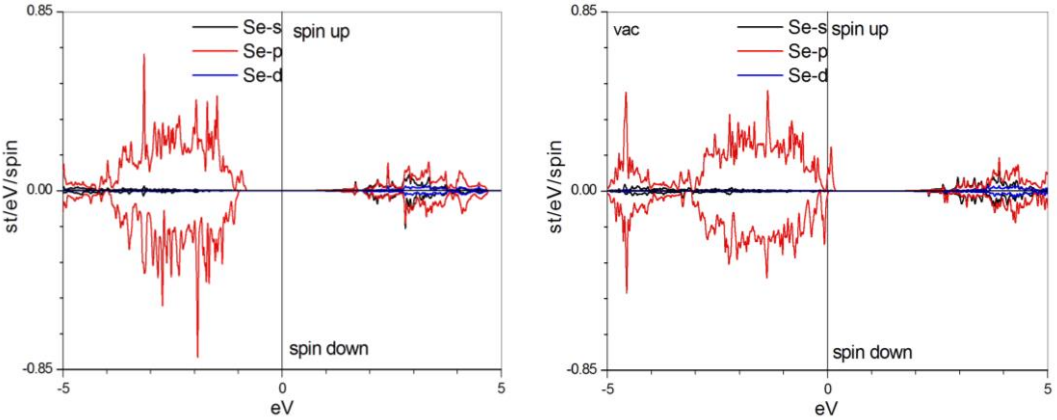

Fig. 4. The Se partial density of electronic states in the Mn:ZnSeS material, without and with V_{Zn} vacancy (vac). Pressure P = 0.

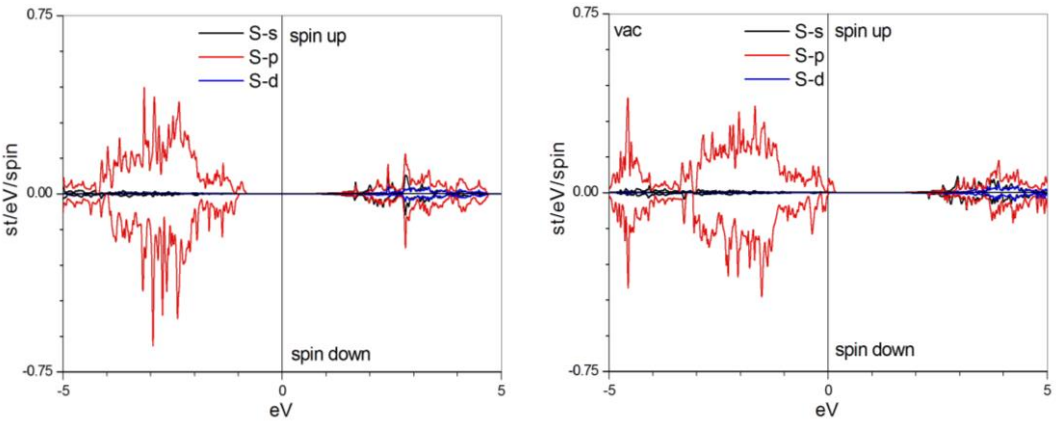

Fig. 5. The S partial density of electronic states in the Mn:ZnSeS material, without and with V_{Zn} vacancy (vac). Pressure P = 0.

P = 23 GPa. A comparison of dispersion laws reveals a significant influence of the V_{Zn} vacancy on the electronic structure of the Mn:ZnSeS material for both spin orientations. In particular, if in the absence of defects the material is a semiconductor for both spin orientations, then in the presence of vacancies it exhibits metallic properties. This conclusion follows from the localization of the Fermi level of the material with vacancies in the upper part of the valence band.

Figure 7 reveals a significant dominance of the 3d electrons of the Mn atom in the valence band as well as in the conduction one. This dominance is characteristic for the material without defects and in the presence of the latter. The material without defects remains in the semiconducting state even in the presence of pressure, but vacancies induce its transition to the metallic state. This is confirmed by the intersection of the density of states curves with the Fermi level.

Figure 8 shows the partial densities of electronic states of the Zn atom. On the left are the curves obtained for the Mn:ZnSeS material under hydrostatic pressure, but without point defects. They correspond to the material in

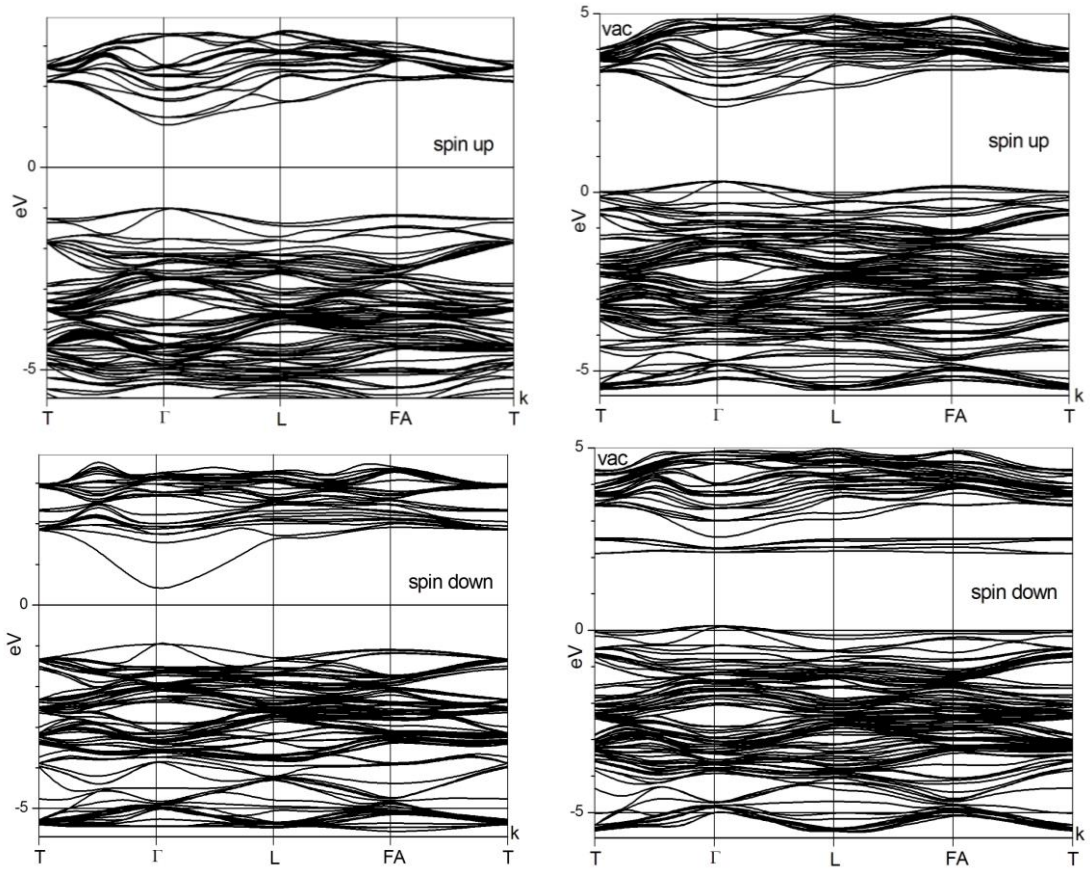

Fig. 6. Spin-polarized electronic energy spectra of the Mn:ZnSeS material, without and with the V_{Zn} vacancy (vac). Pressure P = 23 GPa.

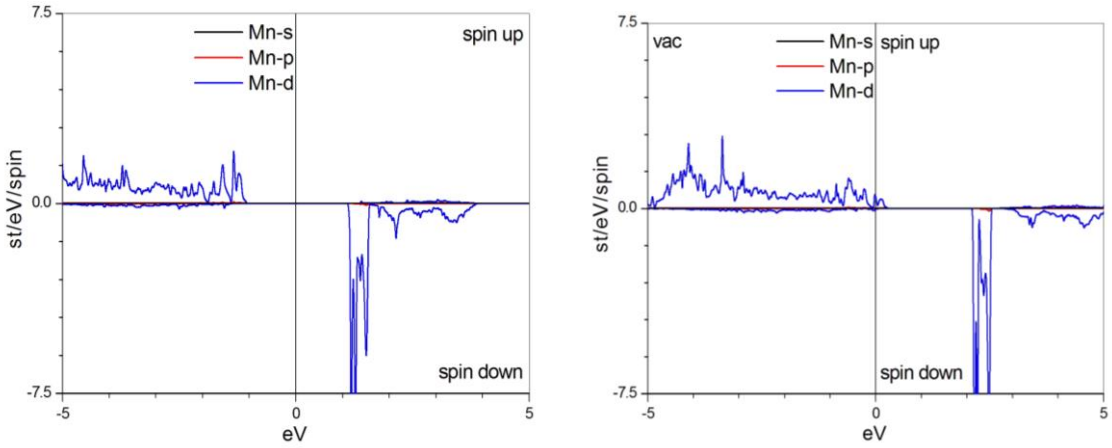

Рис. 7. The Mn partial density of electronic states in the Mn:ZnSeS material, without and with the V_{Zn} vacancy (vac). Pressure P = 23 GPa.

the semiconductor state. On the right are the results found for the material under pressure as well as in the presence of vacancies. The Fermi level is localized at the top of the valence band, so it corresponds to the metallic state.

Fig. 9 shows the partial densities of electronic states of the Se atom. On the left are the curves obtained for the Mn:ZnSeS material under hydrostatic pressure, but without point defects. They correspond to the material in the semiconductor state. On the right are the results found for the material under pressure as well as in the presence of vacancies. The Fermi level is localized at the top of the valence band, so it corresponds to the metallic state.

In fig. 10 shows the partial densities of electronic states of the S atom. On the left are the curves obtained for the Mn:ZnSeS material under hydrostatic pressure, but without point defects. They correspond to the material in the semiconductor state. On the right are the results found for the material under pressure as well as in the presence of vacancies. The Fermi level is localized at the top of the valence band, so it corresponds to the metallic state.

Comparison of the dispersion curves shown in Figures 1 and 6, as well as the densities of electronic states (Figures 2–5, 7–10) reveals that V_{Zn} cation vacancies cause significant changes in the parameters of electronic energy bands. If the external hydrostatic pressure does not lead to a change in the nature of the material, vacancies contribute to the transition of the material from the semiconductor state to the metallic state.

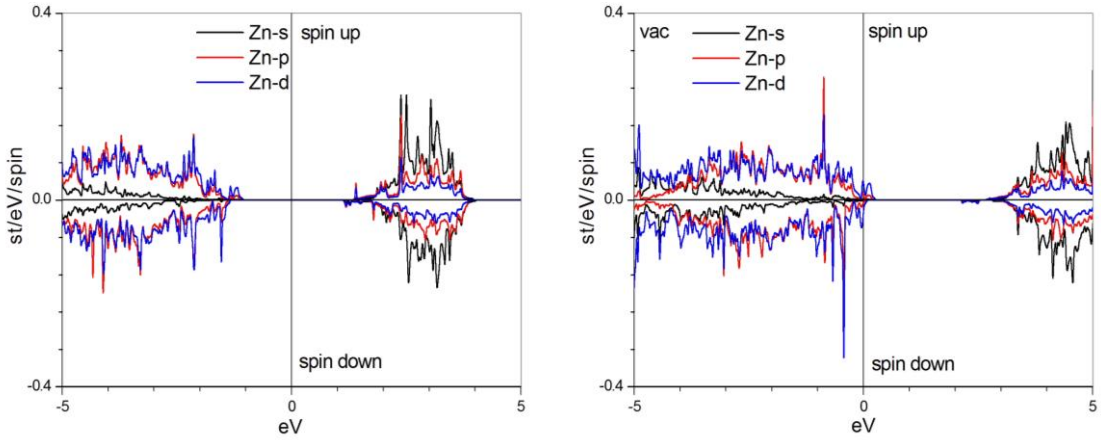

Fig. 8. The Zn partial density of electronic states in the Mn:ZnSeS material, without and with VZn vacancy (vac). Pressure P = 23 GPa.

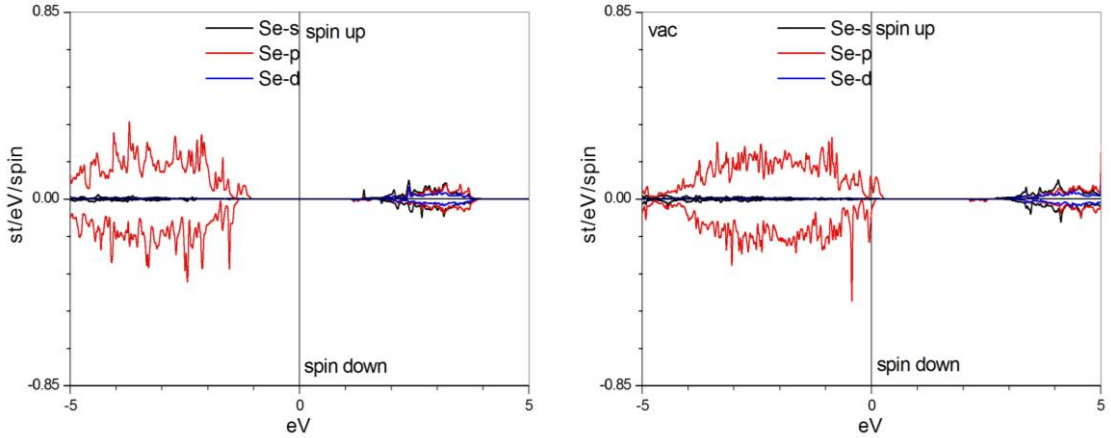

Fig. 9. The Se partial density of electronic states in the Mn:ZnSeS material, without and with V_{Zn} vacancy (vac). Pressure P = 23 GPa.

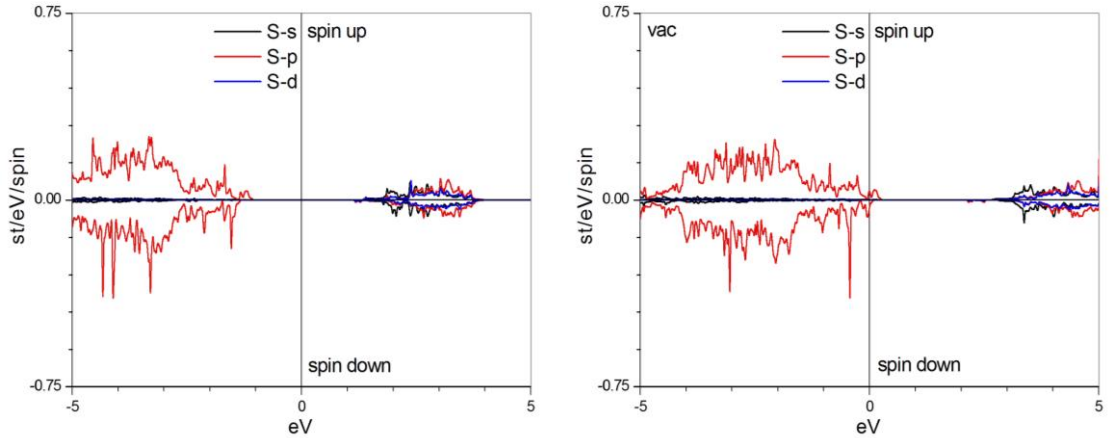

Fig. 10. The S partial density of electronic states in the Mn:ZnSeS material, without and with V_{Zn} vacancy (vac). Pressure P = 23 GPa.

Conclusion

The spin-polarized electronic energy spectra of the Mn:ZnSeS system were obtained for the 2×2×2 supercell. The calculated electronic structure of this material without and with the presence of a point defect – vacancies at the node of the Zn atom. The calculations were performed under normal conditions and in the presence of external hydrostatic pressure. It was found that the 3d electrons of the Mn impurity atom are localized in narrow energy zones with large values of the density of electronic states (DOS).

The electronic structure of the Mn:ZnSeS material without point defects and under normal conditions reveals semiconducting properties for both spin orientations. For electrons with upward spin, the fundamental band gap is

1.6049 eV, and the optical one is 1.6052 eV. For oppositely oriented spin, these parameters are equal to 1.7765 eV and 1.7771 eV, respectively. The magnetic moment of the supercell is 5.0 μ_B, and the contribution of the Mn atom to it is 3.80 μ_B.

The electronic structure of the Mn:ZnSeS material with a vacancy on the Zn atom node (VZn) and under normal conditions reveals metallic properties for both spin orientations. This follows from the fact that the Fermi level is localized in the upper part of the valence band. The magnetic moment of the supercell is 3.98 μ_B, and the contribution of the Mn atom to it is 3.78 μ_B.

The electronic structure of the Mn:ZnSeS material without point defects and under the influence of external hydrostatic pressure reveals semiconducting properties for both spin orientations. For electrons with upward spin, the fundamental and optical band gaps are equal to 2.07 eV. For oppositely oriented spin, these parameters are identical and equal to 2.30 eV. The magnetic moment of the supercell is equal to 5.0 μ_B, and the contribution of the Mn atom to it is 3.60 μ_B.

The electronic structure of the Mn:ZnSeS material with a vacancy on the Zn atom node (VZn) and under the action of external hydrostatic pressure reveals metallic properties for both spin orientations. This follows from the fact that the Fermi level is localized in the upper part of the valence band. The magnetic moment of the supercell is 4.15 μ_B, and the contribution of the Mn atom to it is 3.54 μ_B.

Acknowledgments

This contribution was created under the support of the High Performance Computing Laboratory at the Lviv Polytechnic National University.

Syrotyuk S.V. – PhD, Prof. Assoc., CAS;
Nakonechnyi A.Y. – Dr. Engineering Sci., Head of Computerized Automation Systems (CAS); Department;
Klysko Yu.V. – PhD, Assist. Prof., CAS;
Vlakh-Vyhrynovska H.I. – PhD., Prof. Assoc., CAS;
Veres Z.E. – PhD, Assist. Prof., CAS.

[1] O.G. Trubaieva, M.A. Chaika, A.I. Lalayants, *The growth, structure and luminescence properties of ZnSe1-xSx materials*, Lith. J. Phys., 58(3), 254 (2018); https://doi. org/10.3952/physics.v58i3.3813.
[2] V.A. Litichevskyi, A.D. Opolonin, S.N. Galkin, A.I. Lalaiants, E.F. Voronkin, *A dual-energy X-ray detector on the basis of ZnSe(Al) and LGSO(Ce) composite scintillators*, Instrum. Exp. Tech. 56, 436 (2013); https://doi.org/10.1134/S0020441213040209.
[3] U. Hotje, C. Rose, M. Binnewies, *Lattice constants and molar volume in the system ZnS, ZnSe, CdS, CdSe*, Solid State Sci. 5, 1259 (2003); https://doi.org/10.1016/S1293-2558(03)00177-8.
[4] K.A. Katrunov, A.L. Lalayants, V.N. Baumer, S.N. Galkin, L.P. Galchinetskii, and E.J. Brilyova, *Peculiarities of scintillation materials based on ZnS–ZnTe solid solutions*, Funct. Mat. 20, 384 (2013); https://doi.org/10.15407/fm20.03.384.
[5] Y. Shirakawa, H. Kukimoto, *The electron trap associated with an anion vacancy in ZnSe and ZnSxSe1–x*, Solid State Commun. 34, 359 (1980); https://doi.org/10.1016/0038-1098(80)90575-X.
[6] M.M. Slyotov, O.M. Slyotov, *Preparation and luminescent properties of zinc sulfoselenide thin films*, Phys. Chem. Solid State, 20, 354 (2019); https://doi.org/10.15330/pcss.20.4.354-359.
[7] O.P. Malyk, S.V. Syrotyuk, *Heavy hole scattering on intrinsic acceptor defects in cadmium telluride: calculation from the first principles*, Phys. Chem. Solid State, 23(1), 89 (2022); https://doi.org/10.15330/pcss.23.1.89-95.
[8] H.A. Ilchuk, L.I. Nykyruy, A.I. Kashuba, I.V. Semkiv, M.V. Solovyov, B.P. Naidych, V.M. Kordan, L.R. Deva, M.S. Karkulovska, R.Y. Petrus, *Electron, phonon, optical and thermodynamic properties of CdTe crystal calculated by DF*T, Phys. Chem. Solid State, 23(2), 261 (2022); https://doi.org/10.15330/pcss.23.2.261-269.
[9] A.I Kashuba, B. Andriyevsky, I.V. Semkiv, H.A. Ilchuk, R.Y. Petrus, Ya.M. Storozhuk, *First-principle calculations of band energy structure of CdSe0.5S0.5 solid state solution thin films*, Phys. Chem. Solid State, 23, 52 (2022); https://doi.org/10.15330/pcss.23.1.52-56.
[10] P. Fjodorow, M.P. Frolov, Y.V. Korostelin, V.I. Kozlovsky, C. Schulz, S.O. Leonov, Y.K. Skasyrsky, *Room-temperature Fe:ZnSe laser tunable in the spectral range of 3.7–5.3 μm applied for intracavity absorption spectroscopy of CO2 isotopes, CO and N2O*, Opt. Express, 29(8), 12033 (2021); https://doi.org/10.1364/OE.422926.
[11] K. Karki, S.Yu, V. Fedorov, D. Martyshkin, S. Subedi, Y. Wu, and S. Mirov, *Hot-pressed ceramic Fe:ZnSe gain-switched laser*, Opt. Mater. Express, 10, 3417 (2020); https://doi.org/10.1364/OME.410941.
[12] V.I. Kozlovsky, Y.V. Korostelin, Y.P. Podmar'kov, Y.K. Skasyrsky, M.P. Frolov, *Middle infrared Fe2+:ZnS, Fe2+:ZnSe and Cr2+:CdSe lasers: new results*, J. Phys.: Conf. Ser. 740, 012006 (2016); https://doi.org/10.1088/1742-6596/740/1/012006.
[13] S.V. Syrotyuk, O.P. Malyk, *Effect of Strong Correlations on the Spin-polarized Electronic Energy Bands of the CdMnTe Solid Solution*, J. Nano- Electron. Phys., 11, 01009 (2019); https://doi.org/10.21272/jnep.11(1).01009.
[14] S.V. Syrotyuk, Moaid K. Hussain, *The Effect of Cr Impurity and Zn Vacancy on Electronic and Magnetic Properties of ZnSe Crystal*, Phys. Chem. Solid State: 22, 529 (2021); https://doi.org/10.15330/pcss.22.3.529-534.
[15] S.V. Syrotyuk, M.K. Hussain, *Influence of Pressure on the Electronic and Magnetic Properties of the ZnSeTe Solid Solution Doped with Fe Atoms*, J. Nano- Electron. Phys. 15, 05002 (2023); https://doi.org/10.21272/jnep.15(5).05002.

[16] S.V. Syrotyuk, O.P. Malyk, Yu.V. Klysko, *The influence of pressure on the spin-polarized electronic structure of ZnSeTe:T (T=Cr, Mn, Fe) doped solid solution*, Mol. Cryst. Liq. Cryst., 766, 121 (2023); https://doi.org/10.1080/15421406.2023.2238995.
[17] G. Gulyamov, S.B. Utamuradova, M.G. Dadamirzaev, N.A. Turgunov, M. K. Uktamova, K.M. Fayzullaev, A.I. Khudayberdiyeva, A.I. Tursunov, *Calculation of the total current generated in a tunnel diode under the action of microwave and magnetic fields*, East Eur. J. Phys. 2, 221 (2023); https://doi.org/10.26565/2312-4334-2023-2-24.
[18] X. Gonze et al., *Recent developments in the ABINIT software package*, Comput. Phys. Comm. 205, 106 (2016); https://doi.org/10.1016/j.cpc.2016.04.003.
[19] P.E. Blöchl, *Projector augmented-wave method*, Phys. Rev. B, 50, 17953 (1994); https://doi.org/10.1103/PhysRevB.50.17953.
[20] J.P. Perdew, K. Burke, M. Ernzerhof, *Generalized Gradient Approximation Made Simple*, Phys. Rev. Letters 77, 3865 (1996); https://doi.org/10.1103/PhysRevLett.77.3865.
[21] M. Ernzerhof, G.E. Scuseria, *Assessment of the Perdew–Burke–Ernzerhof exchange-orrelation functional*, J. Chem. Phys. 110, 5029 (1999); https://doi.org/10.1063/1.478401.

С.В. Сиротюк, А.Й. Наконечний, Ю.В. Клиско, Г.І. Влах-Вигриновська, З.Є. Верес

Електронні й магнітні властивості твердого розчину ZnSeS, модифіковані домішкою Mn, вакансією Zn та тиском

Кафедра комп'ютеризованих систем автоматики, Національний університет "Львівська політехніка", Львів, Україна, stepan.v.syrotiuk@lpnu.ua

Поляризовані за спіном електронні енергетичні спектри твердого розчину ZnSeS отримані на основі розрахунків для надкомірки, яка містить 64 атоми. На *першому* етапі підраховані властивості матеріалу на основі надкомірки Mn:ZnSeS, у якій Mn заміщує атом Zn. Результати підрахунку виявляють, що матеріал є напівпровідником для обидвох орієнтацій спіна. *Другий* етап грунтується на одночасній присутності домішки Mn і катіонної вакансії. Порівняння результатів перших двох етапів дозволяє виявити значні зміни електронної енергетичної структури, зумовлені катіонною вакансією. Матеріал з вакансією виявляє металеві властивості для обидвох орієнтацій спіна. *Третій* етап реалізований для надкомірки без вакансії, але під дією гідростатичного тиску. Матеріал виявляє напівпровідникові властивості для обидвох значень спінового моменту. На *четвертому* етапі розглянута надкомірка Mn:ZnSeS з вакансією і під дією тиску. За наявності тиску і вакансії V_{Zn} матеріал ZnMnSeS виявляє металеві властивості для обидвох орієнтацій спіна. Матеріал з вакансією і під дією тиску можна характеризувати як магнітний метал.

Ключові слова: Тверді Розчини AIIBVI, Точкові Дефекти, Тиск, Електронна Структура.